

Chapter 19

A Selected Benchmark for Landslides Susceptibility Assessments in Northern Morocco



Meryem Elmoulat and Lahcen Ait Brahim

Abstract During the past two decades (2000–2020) many studies have been conducted to build strategies as preventing landslides. Most of these approaches are focusing on different methods (statistical, mathematical, and machine learning. . . etc.) for the same study area. In the present research, we are benchmarking the results of our approach at two different geographical areas by using the Frequency Ratio (FR). First, we are comparing robustness between two susceptibility assessments for smaller areas such as Ceuta (257 Km²) and Tétouan-Ras-Mazari (590 Km²) to find out their similarities and their differences. Second, for both areas, we are utilizing the same controlling factors e.g., lithology, landuse, fault density, drainage density, slope degrees, slope aspects, and elevation. Third, we calculated the Prediction Rates (PR) of all factors. Fourth, our results show that three factors (Landuse, Elevation, Lithology for Area-1; in addition to, landuse, elevation, and fault density for Area-2 are sufficient for establishing acceptable LSAs for each area. Fifth, the evaluation process for the models is assessed by Areas Under the Curve (AUC). The accuracy of Models-I is 78.55% and Model- II is 79.25%. Last, our strategy could be an asset for our successors interested in Landslide Susceptibility Assessments (LSAs) in mountains MENA regions.

Keywords Frequency ratio (FR) · Landslides susceptibility assessments (LSAs) · Smaller areas · And northern Morocco

19.1 Introduction

Landslides, both natural and man-made are often the cause of extensive material and human damages. These phenomena represent one of the most serious problems affecting several countries in North Africa (Morocco, Algeria, and Tunisia). Morocco, by its geographical location, is regularly exposed to climate change, the

M. Elmoulat (✉) · L. Ait Brahim
Research Unit GEORISK, LG2E Laboratory, Faculty of Sciences, University Mohammed V
Rabat, Rabat, Morocco

recurrence of drought, the diversity of geological, hydrogeological, and geomorphological nature, which play an instrumental role in the dynamic of triggering Mass Movements (MM). The serious catastrophic events whose impact on the natural environment as well as on human life is nowadays concerned scientists, engineers, and geologists; because of the destructive effect on the economy and human life, which prevents the exploitation of the potential socio-economic development of nations. According to a report published by the Algerian Ministry of agriculture and rural development (Mate, 2004), there are about seven natural hazards have been identified. These risks are usually landslides that influence the development of several Algerian cities. These Mass Movements (MM) led to the destruction of several buildings and the relocation of many families. The volumes of the land involved are highly diverse, depending on the type, depth, activity, and speed of the landslides. The deeper the MM, the more the disaster is damaging. Tunisia is known for landslides that affect its mudstones and marlstone slopes (Maurer, 1976, 1979). According to a definition given by (Marthelot, 1957, 1959), the different types and causes of landslides in Tunisia, are phenomena that can cause substantial damage and significantly harming the well-being of populations by threatening human life (Kassab, 1976, 1979). In Morocco and as mentioned by (Pateau, 2014) many the regions affected by these natural disasters. Rif chain in the northern side of the Kingdom is very active from a geodynamic, geomorphological (ravinement, landslides, etc.), climatic (longer periods of drought in late summer and an intensification of torrential rains in winter) points of view. These traits have led to an increase in risks inherently related to extreme climate change recorded since the 2000s. Moreover, other ingredients are also responsible for MM like economic and socio-demographic growth. Tangier-Tétouan region of the Western Rif is increasingly populated (3,157,075 inhabitants (Haut-commissariat au Plan, 2014)), as it is crossed by newly established communication channels (Mediterranean bypass) and attracts more socio-economic activities.

In this chapter, we will use two study sites in the Tangier-Tetouan region: Ceuta city and Tétouan-Ras-Mazari. More information about these two study areas can be found in our previously published works (Elmoulat & Ait Brahim, 2018, 2020). The present manuscript is crucial to carry out our scientific approach to identifying and assessing landslides susceptibility; in order to minimize the destructive damage of these phenomena. Our choice is justified by the fact that these two sites are integrated into the province of Tetouan, which comes first in the areas severely affected by landslides in Northern Morocco. In explanation, several researchers around the world have conducted benchmarking between many statistical, mathematical, and/or computer learning techniques; in our current study, we focus on leading a Benchmark between two landslides susceptibility assessments (LSAs) of two different geographical areas by using the same statistical approach and the same type of independent factors. This present chapter is organized in four consecutive sections arranged as follows: In the first section (Sect. 19.1), we introduce the research subject that is the mapping of landslides in two different sites using the same

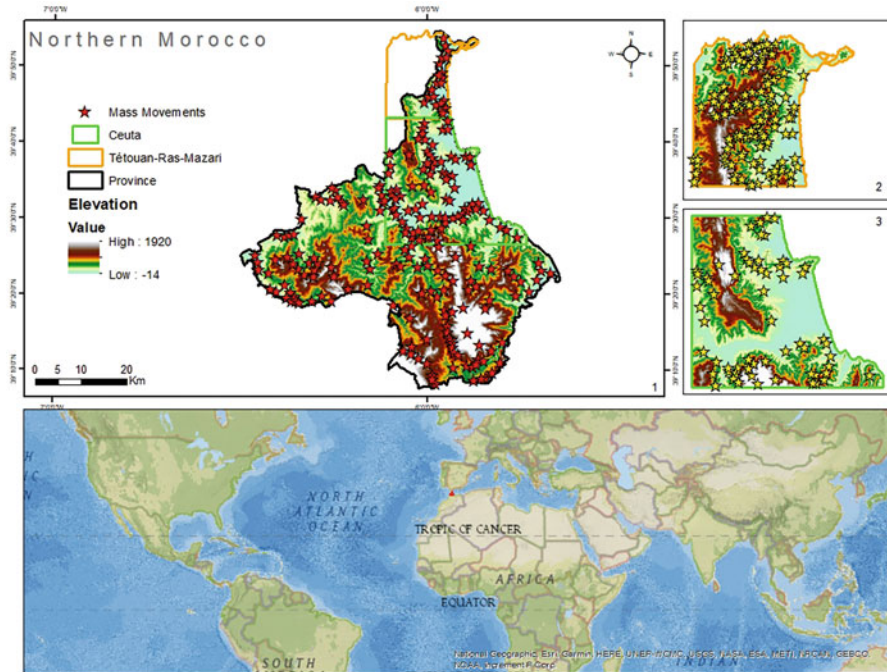


Fig. 19.1 Study areas (Area-1 “Ceuta”, Area-2 “Tétouan-Ras-Mazari”)

statistical approach (FR). In the second section (Sect. 19.2), in which we will explain the procedures and the techniques followed to obtain our desired results. In the third section (Sect. 19.3), we will present our findings. In the fourth section (Sect. 19.4), we provide interpretation and meaning to our previously presented data in the results section. In the fifth section (Sect. 19.5), we conclude and share an overview of our future works (Fig. 19.1).

19.2 Methods and Procedures

In this section, we are going to explain in detail how our questions are answered. This section includes several sub-sections about the implementation of our methodology. First, we provide an overview of our datasets, materials, and sources of our inputs. Second, we explain how we gathered our geodatabase and the preparation process. Third, we talk about technical details concerning the projections and provide useful information related to our data. Fourth, we cite our previous works and summarize the main information regarding the most important inputs of our

modeling, which are the dependents (landslides) and independents factors (seven controlling factors). Fifth, we cite certain beneficial references about the statistical approach employed in this research. Sixth, we calculate the Prediction Rate (PR) of all our controlling factors and in relationship with landslides. Figure 19.2 depicts the detailed flowchart of our methodology to conduct this research.

19.2.1 Datasets Sources and Materials

Remote sensing imagery becomes more important in landslide studies. Comparison of images collected before and after the event gives relevant support to landslide recognition. Landslide inventory data collected from landslide mapping results and historical records can be employed as a database for susceptibility mapping using GIS and statistical approaches. According to our previously published works (Elmoulat & Ait Brahim, 2018, 2020), a summary of the sources of the datasets is provided in the table below (Table 19.1):

Based on our previous research works (Ait Brahim et al., 2002; Elmoulat et al., 2015) and the ones conducted by our predecessors (Mastere et al., 2015) in the Rif Region seven parameters (lithology, fault density, landuse, drainage density, slope degree, slope aspect, and elevation) are mapped to run the two models (Model-I for Area- 1 and Model-II for Area-2). All these parameters are geo-processed in ArcMap environment except for lithology and landuse for the enhancement and the classification are assisted by using Erdas Imagine.

19.2.2 Production of Dependents and Independents Factors

On one hand, approximately 70% (114 centroids) out of 130 total landslides polygons for Ceuta and 70% (123 centroids) out of 165 for Tétouan-Ras-Mazari were used to train each model. On the other hand, 16 and 42 centroids were used to test model-I and Model-II, respectively. Moreover, seven parameters were used in mapping LSAs for both Models, i.e. lithology, landuse, fault density, drainage density, slope degree, slope aspects, and elevation. All thematic maps have been converted to Grid format. The pixel size of each grid is 100 m.

19.2.2.1 Lithology

Landsat ETM + 7 images are a beneficial toolset to discriminate the different spectral properties for lithological units (Ciampalini et al., 2014). They represent a great

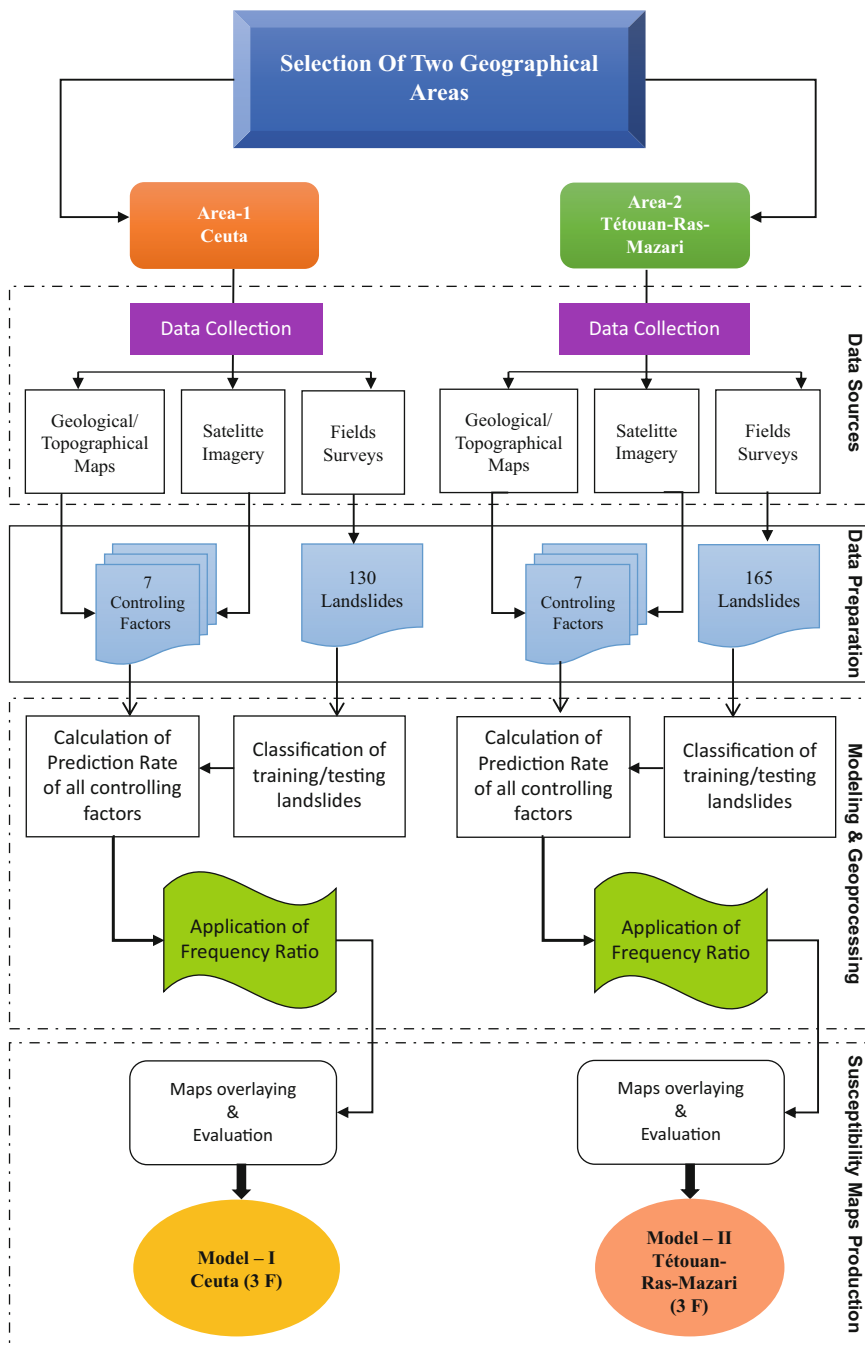


Fig. 19.2 Flowchart of our methodology

Table 19.1 Datasets sources for the two study areas

Data type	Data	Sources	Details
Dependent factor	Landslides	Field surveys	130 landslides for Ceuta and 126 for Tétouan-Ras-Mazari
Independent	Lithology	Satellite imagery: http://earthexplorer.usgs.gov Geological maps: scale of 1/50,000 (Ceuta & Tétouan-Ras-Mazari).	1- LANDSAT ETM+ images consist of seven spectral false-color composites bands with a spatial resolution of 30 m for Bands 1–5, and 7. The resolution for Band 8 (panchromatic) is 15 m. 2- Landsat TM image compose of 6 spectral bands and 1 thermal band (Band 6) with 30 m of spatial resolution.
	Fault density	Satellite imagery: http://earthexplorer.usgs.gov Geological maps: scale of 1/50,000 (Ceuta & Tétouan-Ras-Mazari).	1- LANDSAT ETM+ images consist of seven spectral false-color composites bands with a spatial resolution of 30 m for Bands 1–5, and 7. The resolution for Band 8 (panchromatic) is 15 m. 2- Landsat TM image compose of 6 spectral bands and 1 thermal band (Band 6) with 30 m of spatial resolution.
	Landuse	Satellite imagery: http://earthexplorer.usgs.gov	LANDSAT multi-sensors (TM5, ETM + 7 et ETM + 8), multi-date (1999, 2009, and 2018)
	Drainage density	Digital Elevation Model (DEM) form Shuttle Radar Topography Mission (SRTM): To generate high spatial resolution of 90 meters digital topographic model of the study area. Topographical map: Equidistance contours of 10 meters and scale of 1/50,000.	Sensor: C-band and X-Band Scene size: 1-degree latitude × 1 degree longitude Capture resolution: 1 arc second Pixel resolution: 30 m
	Slope degree	DEM from SRTM	
	Slope aspect	DEM from SRTM	
	Elevation	DEM from SRTM	

source for lithological mapping where access is difficult either for political or geomorphological reasons. For both study sites (Ceuta City and Tétouan-Ras-Mazari), we mapped lithology and classified it into five classes (Figs. 19.3a and 19.4a).

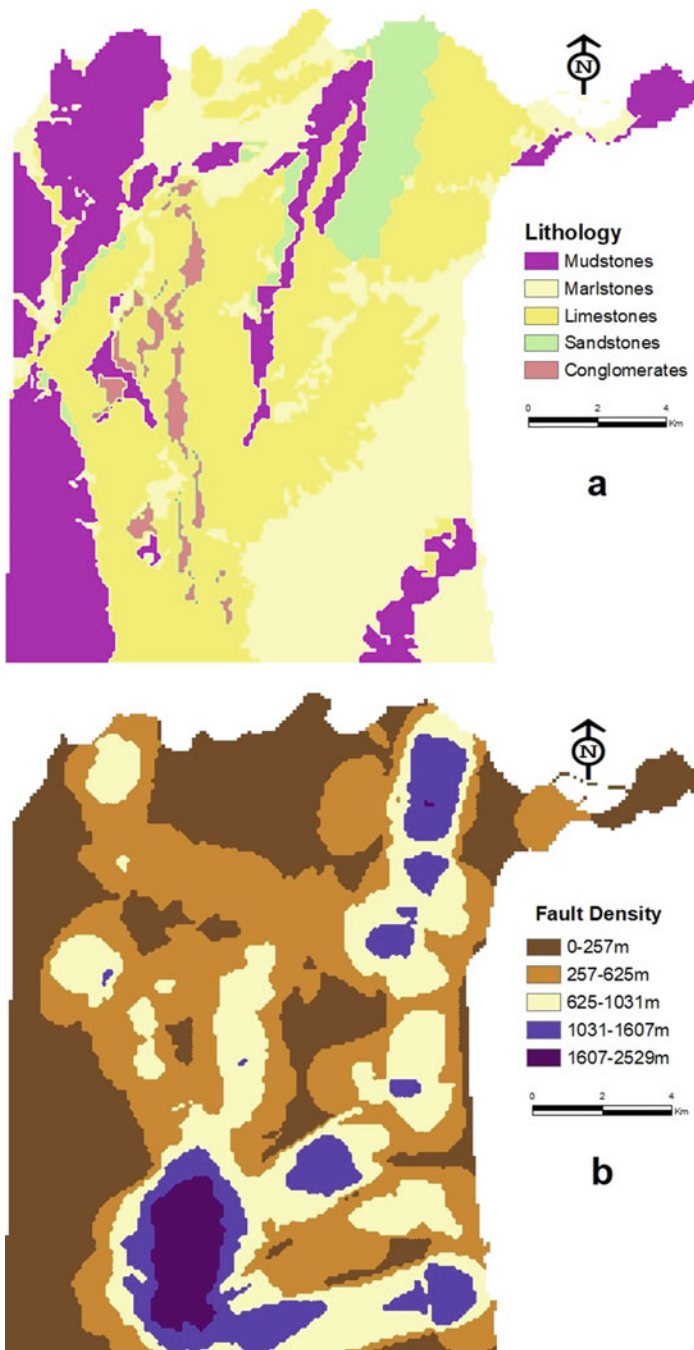


Fig. 19.3 Seven digital thematic maps of the controlling factors of Ceuta City

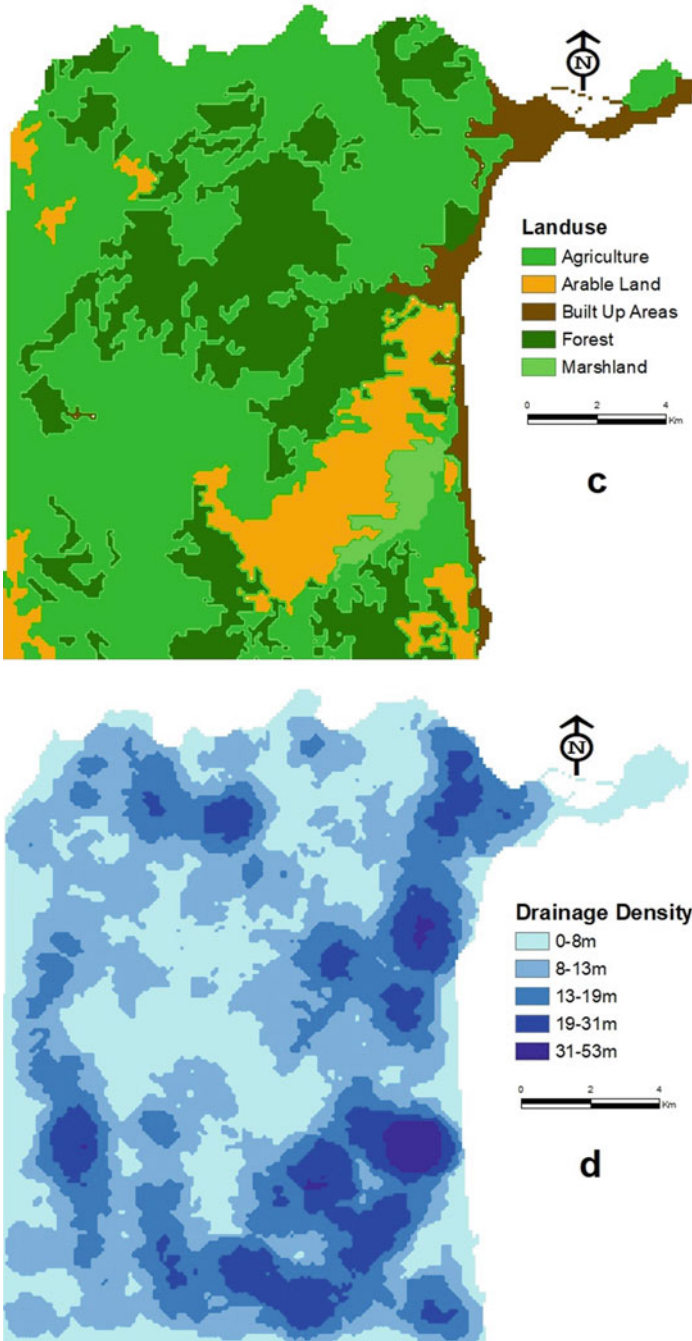


Fig. 19.3 (continued)

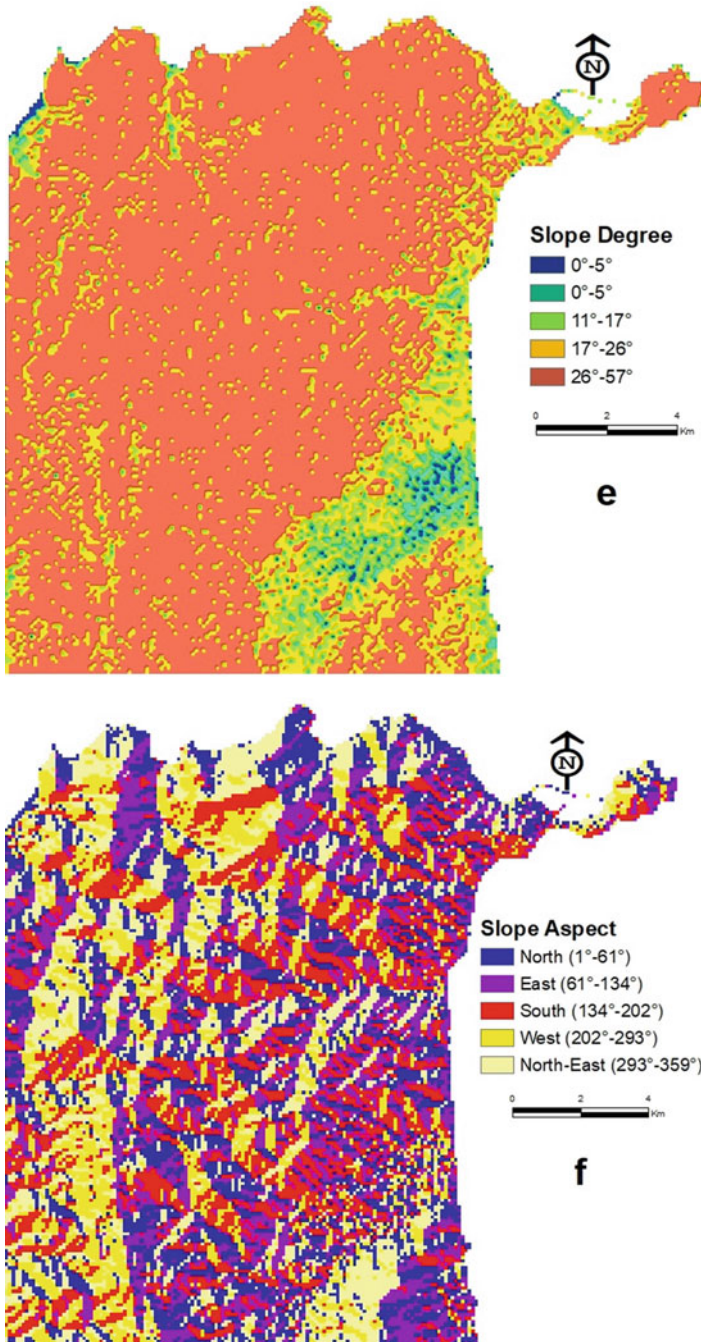


Fig. 19.3 (continued)

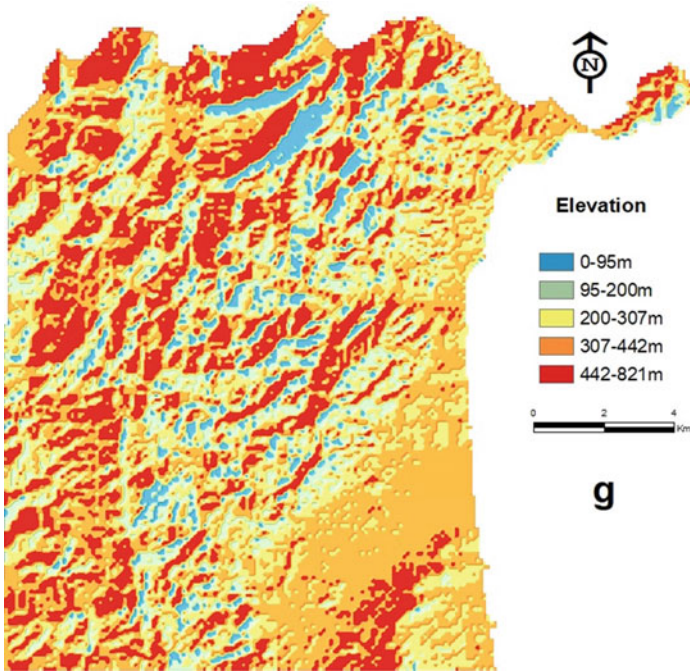


Fig. 19.3 (continued)

19.2.2.2 Fault Density

Experts (Mansour & Ait Brahim, 2005; Shi et al., 2016) in Western Rif have paved the way and allowed us to create faults map for two study areas. Faults maps of Ceuta (Fig. 19.3b) and of Tétouan-Ras-Mazari (Fig. 19.4b) are established by using geological maps, landsat+7, and validated by ground truth studies.

19.2.2.3 Landuse

Vegetation is one of the most prone areas to landslides. The landuse maps have been created based on the supervised classification of ETM+ and validated with field surveys. Figures 19.3c and 19.4c depicts the different classes of landuse factor for Area-1 and Area-2, respectively.

19.2.2.4 Drainage Density

Drainage density was automatically extracted from DEM using ArcHydro tools. The final maps of drainage density were validated using the topographic map of Ceuta and Tétouan-Ras- Mazari (Figs. 19.3d and 19.4d).

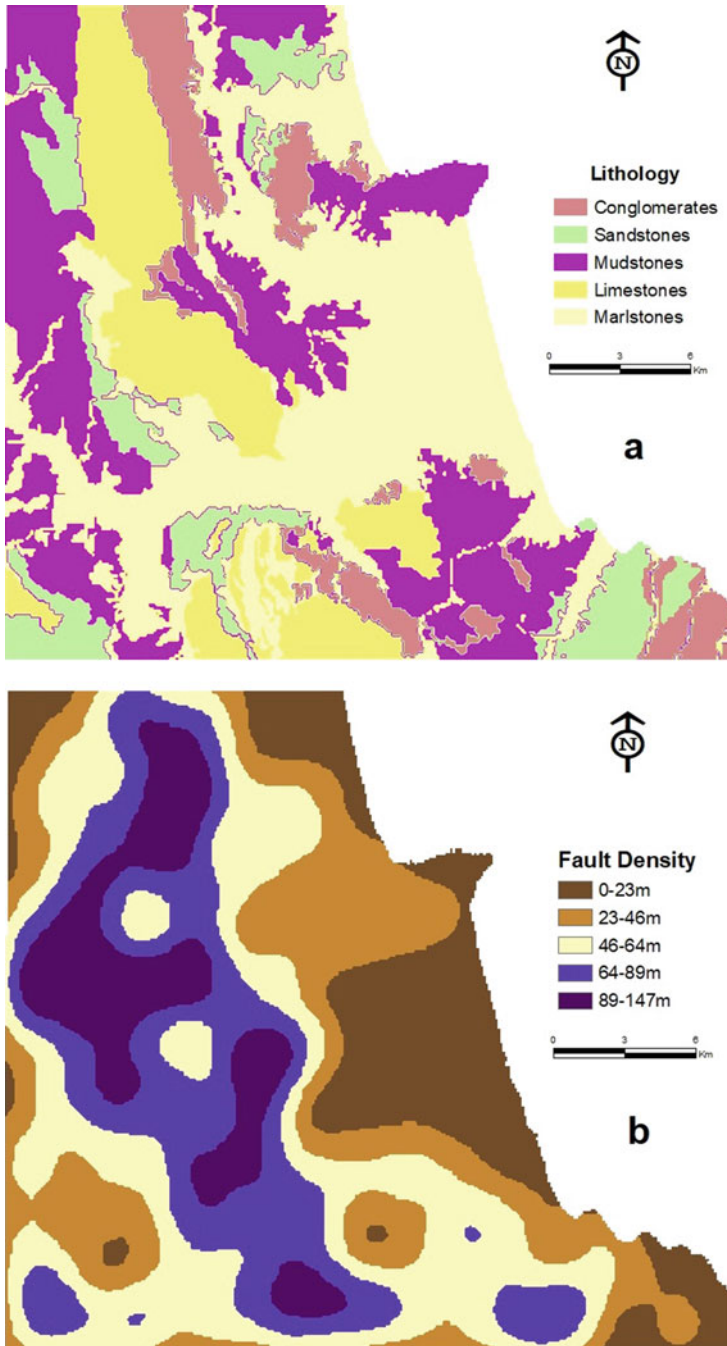


Fig. 19.4 Seven digital thematic maps of the controlling factors of Tétouan-Ras-Mazari

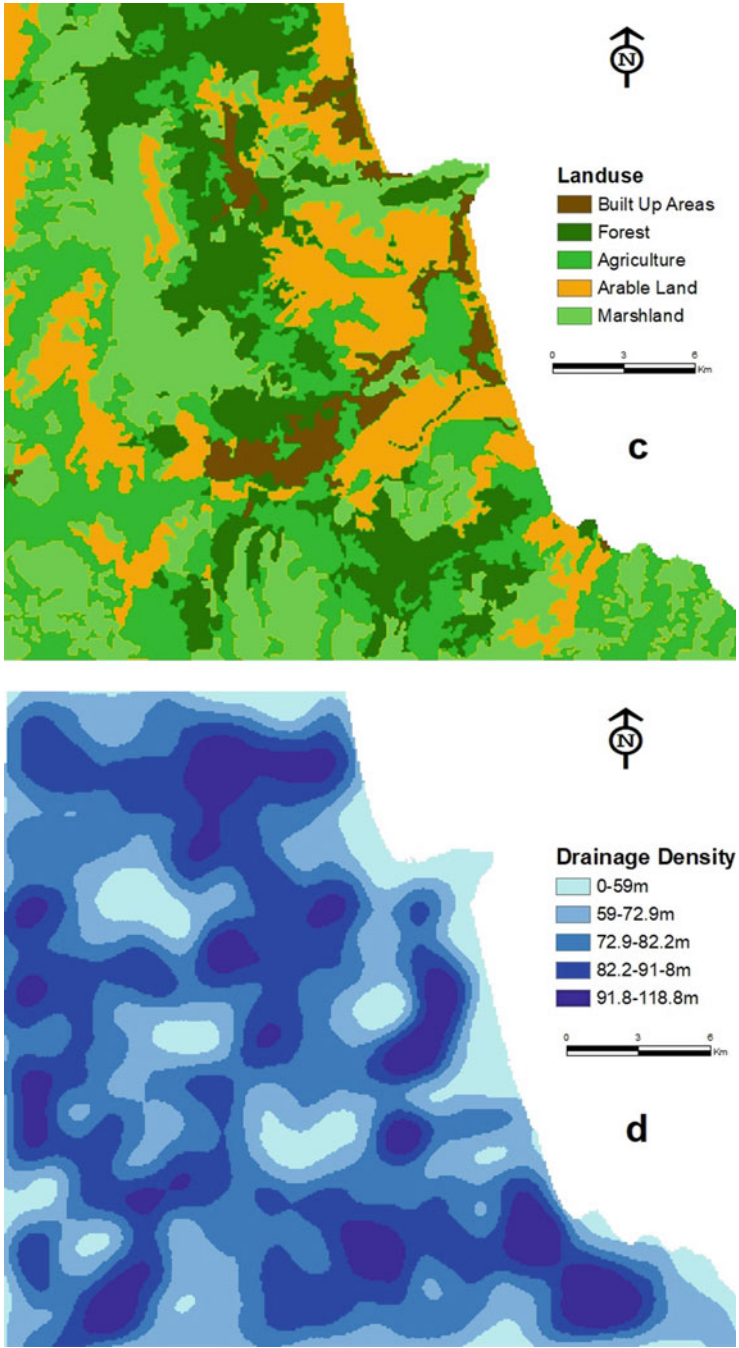


Fig. 19.4 (continued)

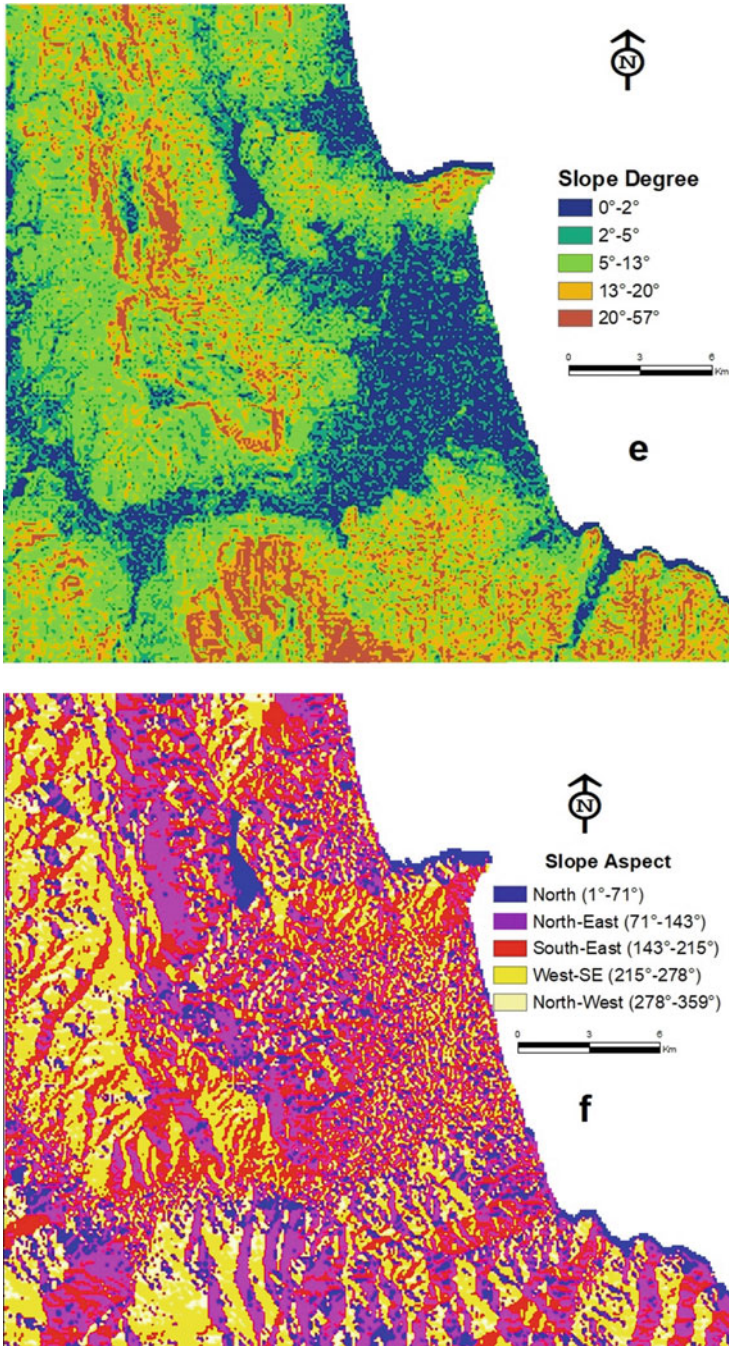


Fig. 19.4 (continued)

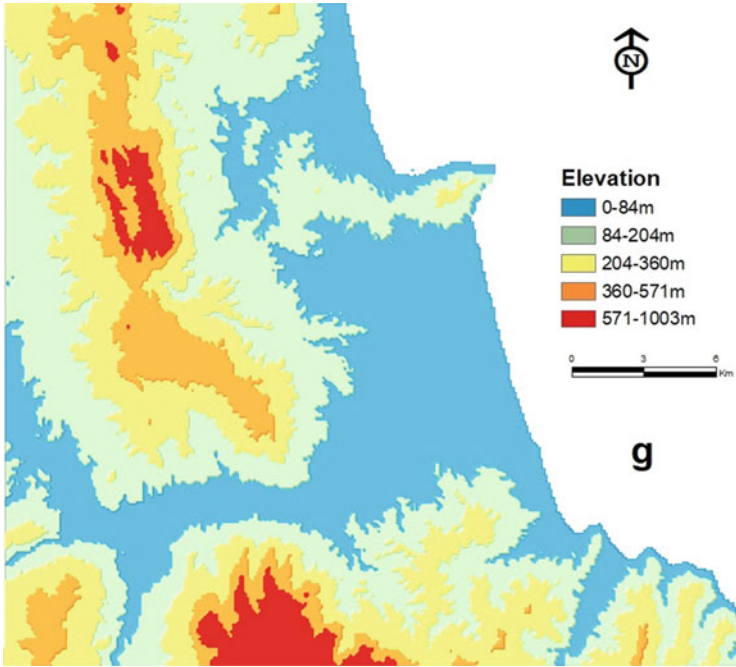


Fig. 19.4 (continued)

19.2.2.5 Slope Degrees

Several authors (Lee, 2019) suggested that slope degrees are mandatory for LSAs. Digital Elevation Model (DEM) extracted from Shuttle Radar Thermometer Mission (SRTM) of 30 m spatial resolution covering our study areas was a useful source to create slope degree maps (Figs. 19.3e and 19.4e).

19.2.2.6 Slope Aspect

The parameter indicates the orientation of the surface that faces at a specific location. Slope aspects maps are considered as a topographical factor that was assessed by using the DEM of the study areas. Figures show slope aspect maps for Ceuta and Tétouan-Ras- Mazari, respectively. of.

19.2.2.7 Elevation

Elevation represents used for points above the surface in each altitude. It used to measure the relationship between altitude above sea level and areas prone to

landslides. Elevation maps for Area-1 and Area-2 are created by using the DEM and they are given by Figs.

19.2.3 Relationship Between Dependents and Independent Factors

To better understand the relationship of all the independent factors with landslide occurrences, we create Pie charts for Area-1 (Fig. 19.5) and for Area-2 (Fig. 19.6). We provide an explanation and interpretation of all the scientific reasoning behind these figures in the discussion section.

19.2.4 Method of Landslides Susceptibility Assessment

According to a review article written by (Nicu, 2017) who conducted a survey based on 776 articles during the last two decades (1999–2018), 24.7% of total articles used Frequency Ratio (FR) to produce GIS-based landslide Susceptibility Mapping. In addition to that, many authors (Kim et al., 2018; Chen et al., 2019; Zhou et al., 2016), proved that FR predicts great results in terms of landslide assessment. In other terms, this statistical approach depicts the relationships between landslides' occurrence in the past and landslides controlling factors. This being said, the greater the ratio is, the stronger the relationship between the landslides and the controlling factors can be (Kirat, 1993). For these reasons and more, we are implementing the same method as our previous research conducted over Ceuta city (Elmoulat & Ait Brahim, 2020) to map landslides susceptibility for two different areas at local scales (Area-1) and (Area-2). All the calculated values mainly ratio, FR, the absolute difference between the maximum and minimum SA values and PR for all factors and for both areas are given in Tables 19.2 and 19.3 below. More information about the equations and how we conducted our calculation can be found in (Elmoulat & Ait Brahim, 2020).

Figure 19.7 depicts the PR of each factor for both models from low to the highly predicted.

19.3 Results

This section is dedicated to only the presentation of our results. Any reading/interpretation is provided in the discussion section.

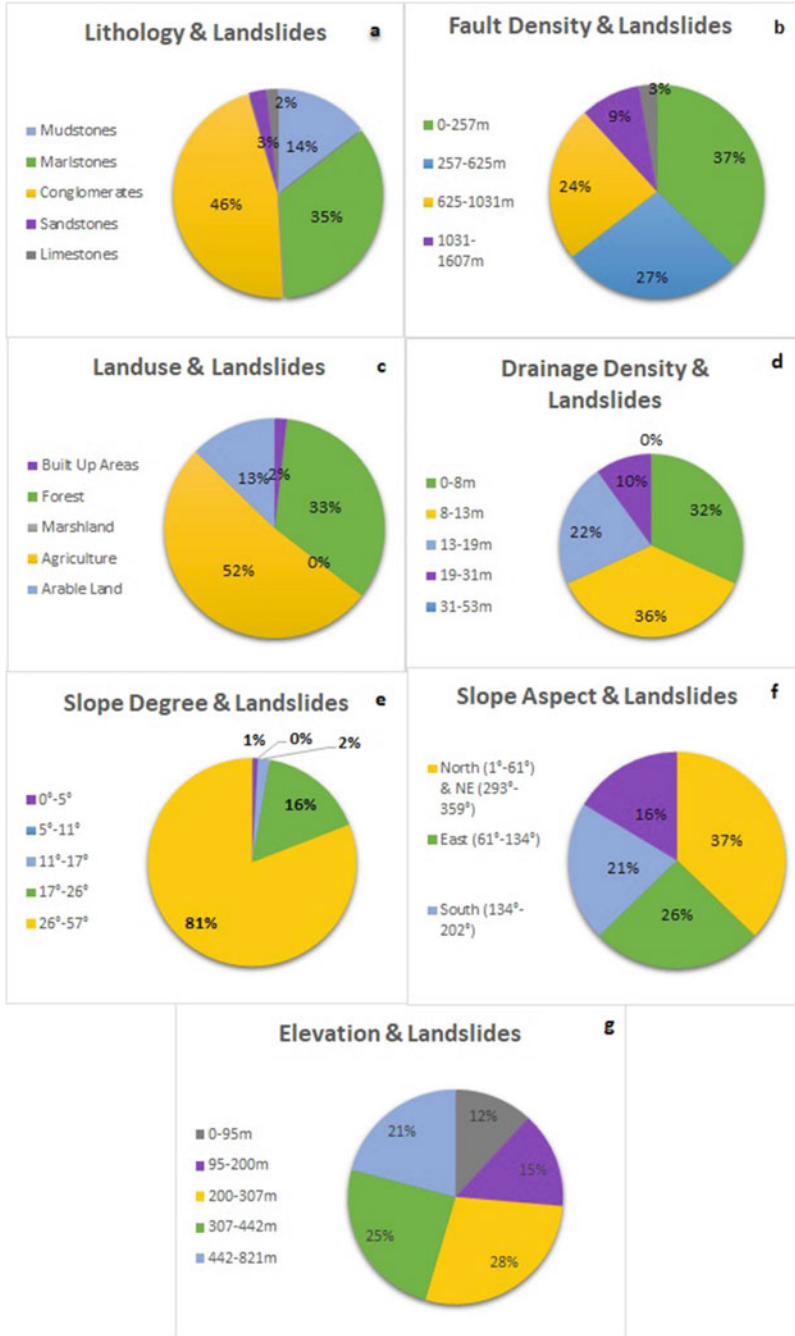


Fig. 19.5 Percentage of relationships between landslides and seven controlling factors for Ceuta City

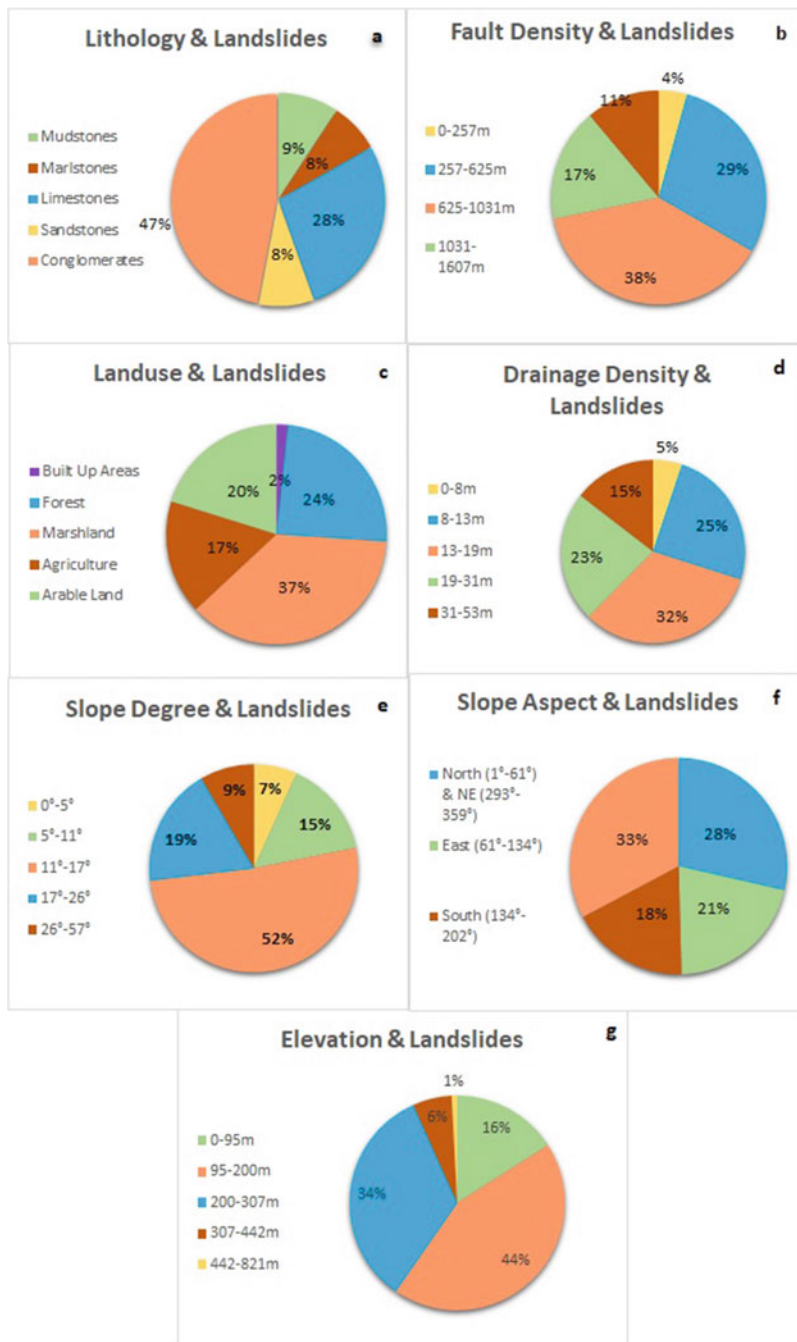


Fig. 19.6 Percentage of relationships between landslides and seven controlling factors for Tétouan-Ras-Mazari

Table 19.2 Ratios and Prediction rates for all the controlling factors of Model-I

Factors and Calsses	Ratio	FR	Min RF	Max RF	[Max- Min]	PR
Lithology			0.11	0.3	0.19	3.8
Mudstones	0.62	0.15				
Marlstones	1.28	0.30				
Limestones	1.13	0.27				
Sandstones	0.47	0.11				
Conglomerates	0.72	0.17				
Fault Density			0.18	0.23	0.05	1
0–257 m	1.15	23.02				
257–625 m	0.80	15.98				
625–1031 m	1.11	22.32				
1031–1607 m	1.03	20.61				
1607–2529 m	0.90	18.07				
Landuse			0	0.33	0.33	6.6
Built up areas	0.37	0.10				
Forest	1.17	0.33				
Marshland	0.00	0.00				
Agriculture	0.98	0.27				
Arable land	1.09	0.30				
Drainage Density			0	0.25	0.25	5
0–8 m	1.01	0.25				
8–13 m	1.01	0.25				
13–19 m	1.01	0.25				
19–31 m	1.00	0.25				
31–53 m	0.00	0.00				
Slope Degree			0	0.33	0.33	6.6
0°–5°	1.19	0.33				
5°–11°	0.00	0.00				
11°–17°	0.30	0.08				
17°–26°	0.98	0.27				
26°–57°	1.10	0.31				
Slope Aspect			0.17	0.25	0.08	1.6
North (1°–61°)	0.84	0.17				
East (61°–134°)	1.26	0.25				
South (134°–202°)	0.99	0.20				
West (202°–293°)	1.02	0.20				
North-East (293°–359°)	0.92	0.18				
Elevation			0.12	0.36	0.24	4.8
0–95 m	2.17	0.36				
95–200 m	0.95	0.16				
200–307 m	1.29	0.22				
307–442 m	0.75	0.12				
442–821 m	0.84	0.14				

Table 19.3 Ratios and prediction rates for all the controlling factors of Model-II

Factors and calsses	Ratio	FR	Min RF	Max RF	[Max–Min]	PR
Lithology			0.11	0.29	0.18	1.72
Conglomerates	1.03	0.23				
Sandstones	0.69	0.15				
Mudstones	1.02	0.22				
Limestones	0.48	0.11				
Marlstones	1.33	0.29				
Fault Density			0.05	0.30	0.25	2.40
0–23 m	0.24	0.05				
23–46 m	1.28	0.27				
46–64 m	1.42	0.30				
64–89 m	0.83	0.18				
89–147 m	0.91	0.19				
Landuse			0.07	0.29	0.33	3.16
Built up areas	0.33	0.07				
Forest	1.23	0.28				
Agriculture	1.29	0.29				
Arable land	0.82	0.19				
Marshland	0.77	0.17				
Drainage Density			0.10	0.30	0.25	2.39
0–59 m	0.50	0.10				
59–72.9 m	1.10	0.22				
72.9–82.2 m	1.06	0.21				
82.2–91.8 m	0.86	0.17				
91.8–118.8 m	1.49	0.30				
Slope Degree			0.09	0.30	0.30	2.89
0°–2°	0.41	0.09				
2°–5°	0.85	0.19				
5°–13°	1.36	0.30				
13°–20°	0.97	0.21				
20°–57°	0.93	0.21				
Slope Aspect			0.15	0.25	0.10	1
North (1°–71°)	1.22	0.24				
North-East (71°–143°)	0.76	0.15				
South-East (143°–215°)	0.80	0.16				
West-SE (215°–278°)	1.30	0.25				
North-West (278°–359°)	1.04	0.20				
Elevation			0.05	0.36	0.31	2.93
0–84 m	0.53	0.13				
84–204 m	1.28	0.31				
204–360 m	1.50	0.36				
360–571 m	0.63	0.15				
571–1003 m	0.23	0.05				

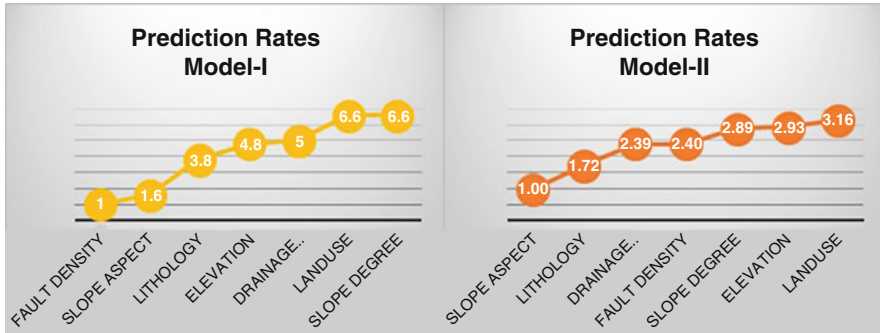


Fig. 19.7 Prediction rates curve of all the controlling factors for Model I (Ceuta) and for Model II (Tétouan-Ras-Mazari)

19.3.1 Model-I (Area-1 Ceuta)

The results to extract from the abovementioned data in the methods section allow us to create landslides Susceptibility Assessment for Ceuta City (Fig. 19.8). Among multiple tests to create the most predictable model we used the highly predicted factors and conditionally independent, which are landuse, elevation, and lithology for Ceuta City. Afterward, we classified the final map into five classes as not susceptible, low, moderate, high, and very high by using Jenks Natural breaks classification method of ArcMap.

19.3.2 Model-II (Area-2 Tétouan-Ras-Mazari)

The susceptibility map of Area-2 (Tétouan-Ras-Mazari) applied the same rule of the selection of controlling factors as stated in previous part 3.1, which are landuse, elevation, and fault density. Figure 19.9 depicts the final LSA of Tétouan-Ras-Mazari.

19.3.3 Models Validation

To understand the area of each subclass of both LSAs, we create the graphs in Fig. 19.10. More reading of these graphs are provided in the discussion section.

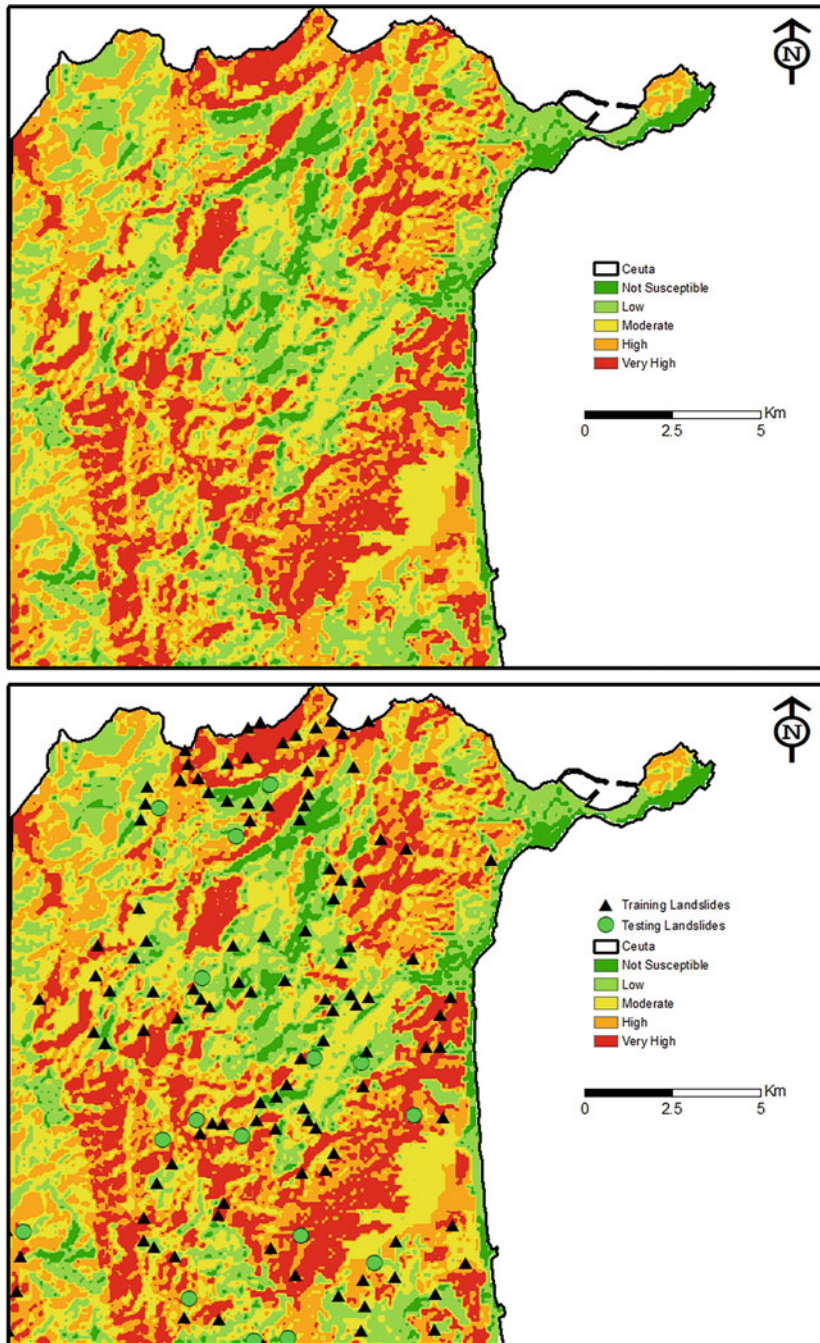


Fig. 19.8 Landslides susceptibility assessment of Ceuta City

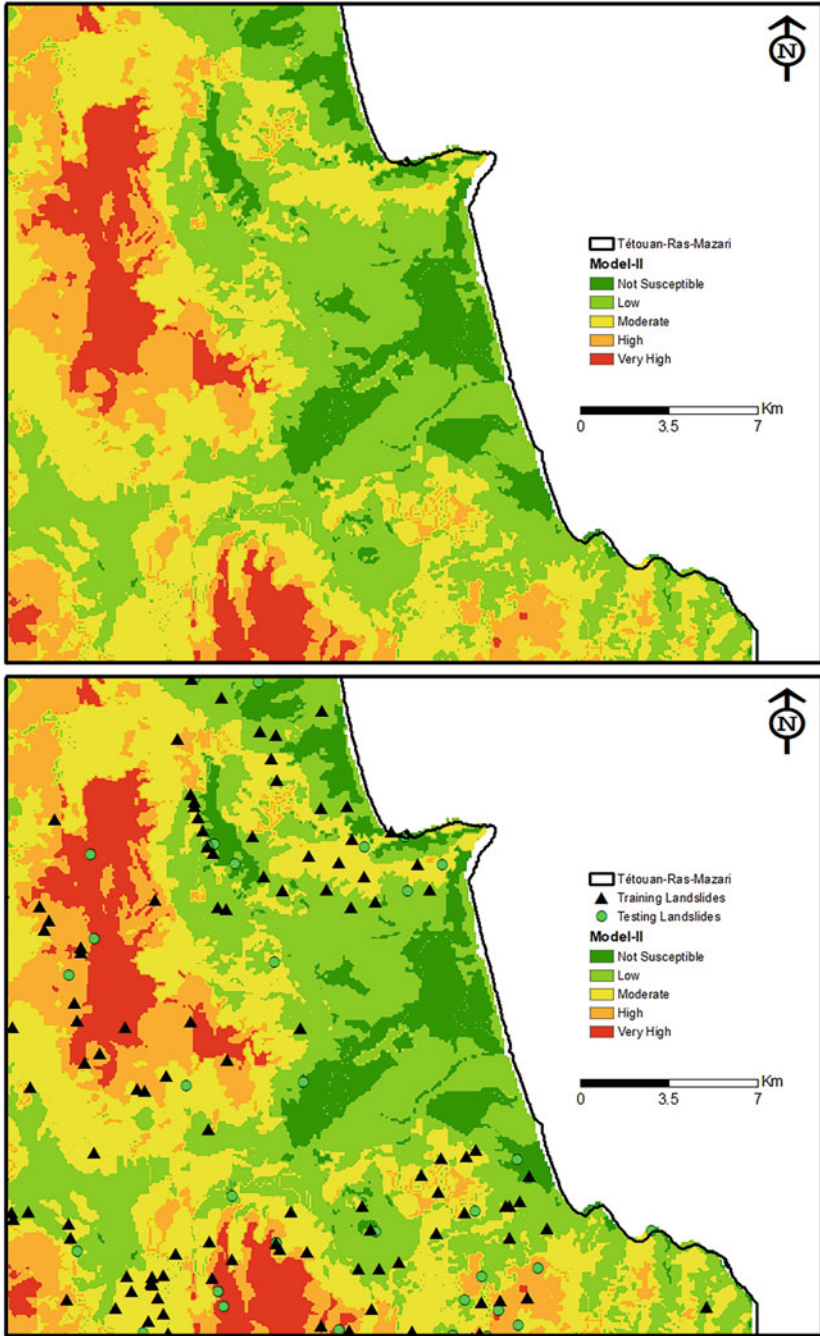


Fig. 19.9 Landslides susceptibility assessment of Tétouan-Ras-Mazari

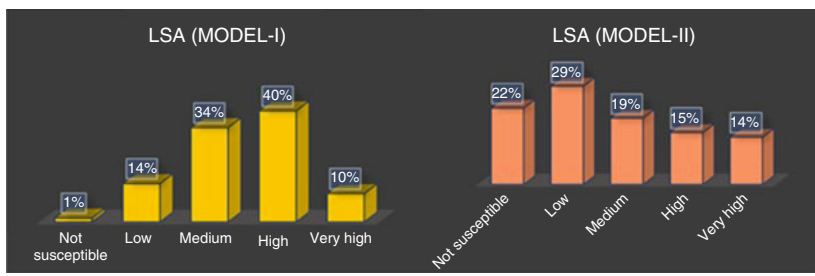
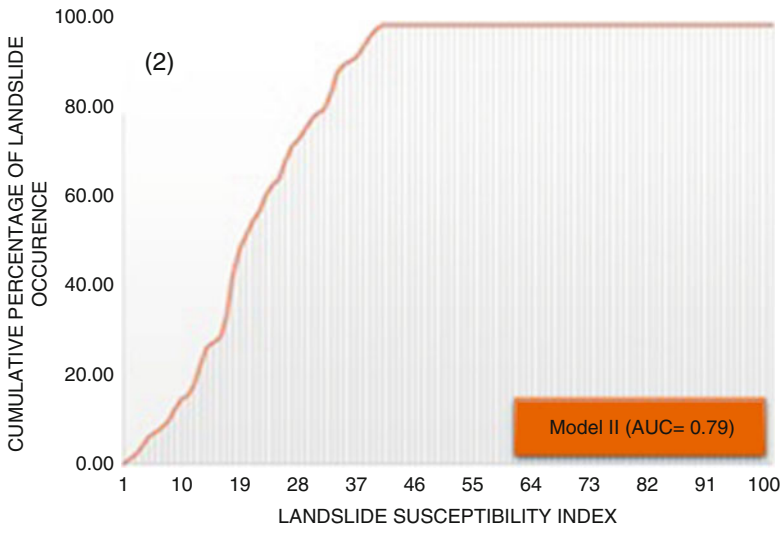
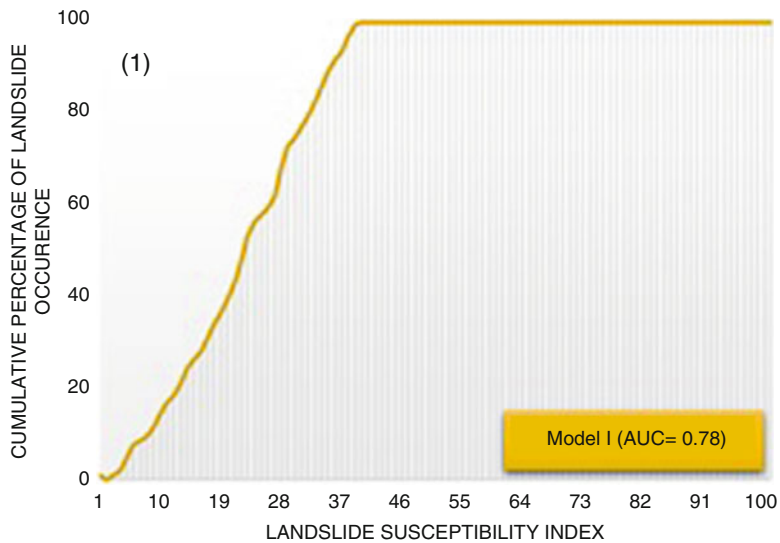


Fig. 19.10 Areas percentages for LSAs for Area-1 and Area-2

Receiver operating characteristic (ROC) or Area Under Curve (AUC) is well known for its capability to predict the accuracy of a model based on presence and absence of a series of data. AUC of our Models are given by Fig. 19.11.

The percentages of cross-validation between the results of LSAs and the testing data are shown in the Fig. 19.12.

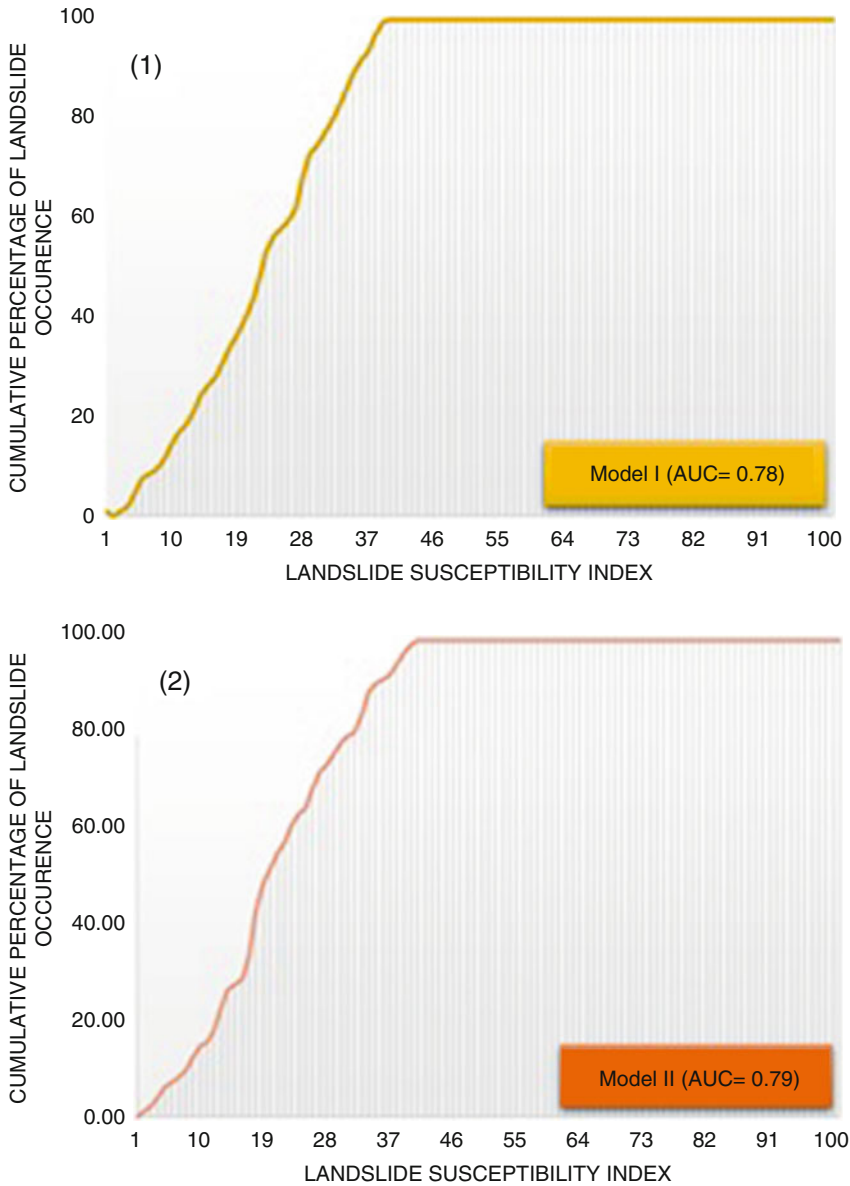


Fig. 19.11 AUC for model-I (1) and for Model-II (2)

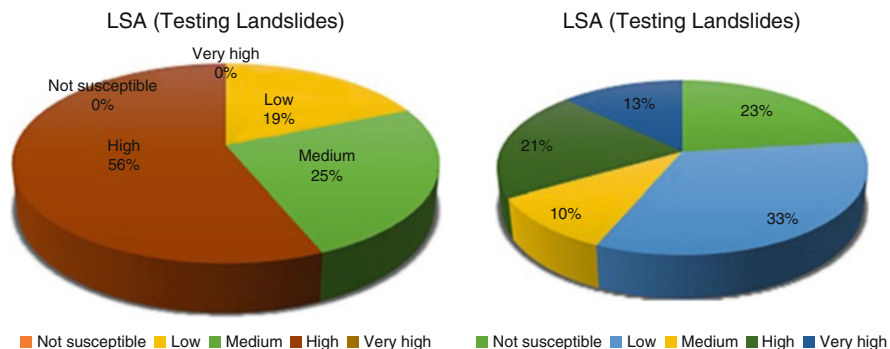


Fig. 19.12 Results of cross-validation between the results of LSAs and the testing data

19.4 Discussions

19.4.1 Relationship Between Landslides and Controlling Factors

According to the results of our analysis shown in the Figs. 19.5 and 19.6, the most striking findings to emerge from the relationship between landslides’ occurrence and the explanatory factors used to predict the LSA are discussed as follow:

19.4.1.1 Landuse

The relationship between landuse and mass movement, specifically rock falls in Ceuta city and landslides in Tétouan-Ras-Mazari are shown in Figs. 19.5c and 19.6c. This type of mass movements are very abundant in agricultural land with 53%, and in the forests subclass 34% for Ceuta City. Concerning Tétouan-Ras-Mazari, the highest percentage exhibits 37% of landslides in marshland and 24% in forest. There are several possible explanations for this result. First, we are concerned about the quality of the agricultural land in Ceuta area and marshland in Tétouan-Ras-Mazari. If these two subclasses of landuse are prone to rock falls/landslides; so probably the top layer of soil is removed due to soil erosion; which is a natural process caused by the weather that harms the agricultural land. Second, we observe that the subclass of forest is also conducive to the outbreak of rock falls in this portion of the study area. Unexpectedly, forest stabilizes the equilibrium of land and therefore increases the shearing strength. However, this is not particularly surprising given the fact that a clear impact of rockfalls on forest is observed. As matter of fact, dendrochronology can show a past effect, with missing of trees’ competent. To better understand the relationship between rock falls and the forest, a further macroscopic section can be used for dating rockfalls events (16).

19.4.1.2 Elevation

By looking at the Figs. 19.5g and 19.6g, we notice the relationship between MM occurrence and altitude. They show that in Ceuta moderate and high altitudes represent 28%(200–307 m) and 25% (307–442 m) respectively. This result reflects the direct relationship between MM occurrences and high altitudes. Regarding Tétouan-Ras-Mazari the two highest percentage are 44% (for low altitude (95–200 m) and 34% for medium ones (200–307 m). Thus, it can be conceivably hypothesized due to the road cutting and human activities in unstable slopes.

19.4.1.3 Fault Density & Lithology

The third factors used in our models are conditionally dependent for two different geographical areas and therefore we will be discussed them separately:

For Area-1, lithology is considered as the third highly predicted factor. Figure 19.5a reveals that conglomerates exhibits 46% of MM and marlstones 35% of MM. These values are consistent with previous results (Ait Brahim et al., 2002; Ait Brahim & Sousse, 2003; Kirat, 1993). Consequently, rock falls are intimately related to the conglomerates and marlstones of Flysch Nappes. Concerning Area-2, Fault density is the third predicted factor. Figure 19.6b provides the results of this class. We notice that highest percentage is attributed to middle class 38% (625 m–1031 m) and next comes the low class (257–625 m) that represent 28% of total MM. This expectation lends to support the general rule that the probability of landslides' occurrence increases when the fault density decreases.

19.4.2 Investigation of Landslides Susceptibility Assessment (LSA)

19.4.2.1 Model-I

Investigation of our findings throughout Figs. 19.8 and 19.10 (left) highlights that our model predicts 40% of high susceptible areas and 10% of very high ones of the total study area by using training data and three conditionally independent factors (Landuse, fault density, elevation and). In addition to that, we conduct another analysis to strengthen our confidence about the accuracy of our model and cross-validate the result of susceptibility assessment by using 30% of testing data and the statistic results shown in Fig. 19.12 (left). Our model predicts 56% of the total study area as highly susceptible. To better evaluate our model, we calculate the ROC or AUC. This test forecasts 78%.55 of landslides' occurrence. This is in a good alignment with previous findings in literature. As mentioned by (Chen et al., 2019): "AUC values between 0.7 and 0.9 indicated reasonable agreement". These findings allowed us to recommend that at smaller areas such as Ceuta city three

conditionally independent factors are barely enough to predict risky areas in Northern Morocco.

19.4.2.2 Model-II

Inspection of susceptibility assessment map of Tétouan-Ras-Mazari (Fig. 19.8), statistical analysis, and prediction rate (Fig. 19.10 (left)) of this model highlights the following results:

On one hand, the susceptibility areas of the total study area are 22%, 29%, 19%, 14%, and 15% for the five classes that are not susceptible, low, medium, high, and very high; respectively. Unexpectedly, this can be explained by the high number of active landslides used to run the model (123). On the other hand, the results gathered from the analysis by using testing data. Figure 19.12 (right) highlights that 13% of very high and 21% of high areas. Contrary to expectations, this test overestimated low class and predicted 33% of the total areas. It is plausible that a number of limitations may influence the results obtained. This limitation may be related to the exact ratio of active landslides used for training/testing data. In our previous research (Elmoulat & Ait Brahim, 2018), we used a ratio of 50% of training and 50% of testing and the current model a ratio of 70% of data to run the model and 30 for validation purpose. In terms of the success rate curve, the success rate of the model is 79.25%, which is the highest value found in our analysis among four different tests using only the highly predicted factors (Figs. 19.11 and 19.2). This result shares a number of similarities with (Corona et al., 2017). Hence, we can conclude that three controlling factors which area land use, elevation, and fault density exert more power in triggering landslides in Area-2.

19.4.3 Comparison Between Model-I vs Model-II

In terms of results obtained from the AUC (Fig. 19.11) and the statical analysis conduct by using training and testing data (Figs. 19.10 and 19.12), we conclude that the two areas have two similar predicant factor that are landuse and elevation. The geographical area inserted in the same Rif region and therefore shares that same type of land covers; in addition to that in term of elevation they are slightly different. For area-1 the high rate is observed in the highest class (307–442) because of the geographic location up to the North of the African plate. Concerning area- 2 the highest class is slow class (84–204). This can be explained by the geographical location of area-2 compared to the one of area-1. Thirdly, Model-I used lithology as the third factor to predict susceptible areas, which is crucial because marlstones and conglomerates are dominant formation in area-1. From petrographic and structural point of view, these elements trigger landslides in the Rif region (Shi et al., 2016, Corona et al., 2017). Furthermore, Model-II called out fault density. In our previous works (Elmoulat and Ait Brahim Elmoulat & Ait Brahim, 2018) and field

observations density around 0 m and 60 m are areas prone to mass movements. Our current observation is in complete agreement with our earlier findings. We would like to mention that faults zones between the Flysches Nappes and Tangier Unit highlight an important number of mass movements.

19.5 Conclusion

The present research composes of two different models to create Landslides Susceptibility Assessment (LSA) of two distinct geographical areas (Ceuta City and Tetouan-Ras-Mazari). Both LSAs are implemented by using the Frequency Ratio approach. The factors used in these models based upon the prediction rates of each controlling factor of landslides' occurrences. We selected only conditionally independent parameters whose Prediction Rates (PR) are highly classified. Indeed, conditional dependence decreases the overall accuracy of any model. Our findings reveal that landuse and elevation are major controlling factors for both models. Lithology exerts more power over Ceuta City and fault density takes the deal for Tetouan-Ras-Mazari. The overall accuracy of the two models are evaluated by AUC and cross-validation by using the testing data, which are in reasonable agreement with our predecessors.

The hypothesis of the current research is primarily focused on benchmarking two susceptibility assessments for two smaller areas to determine their main similarities and differences and then gain new knowledge based upon our findings. We are aware that our results cannot be generalized, given the fact that both areas are geographically located in the same meridians, despite the distinct position of their parallels.

To further our research, we plan to extend our studies in several different regions in the world; in totally different locations (countries and why not continents). For instance, we would like to conduct another benchmarking, as soon as we collect the necessary data to do so, between susceptibility maps of areas located, for example, in Asia and/or South American; in addition to the ones already established in North Africa. The knowledge we may acquire from this research, will improve our understanding of global landslides' susceptibility mapping.

In the end, we believe in a famous saying by a Philanthropist, Petra Nemcova: *"We cannot stop natural disasters, but we can arm ourselves with knowledge: so many lives wouldn't have to be lost if there was enough disaster preparedness."* (Nemcova, 2021).

Acknowledgments The authors are extremely grateful and thankful to:

- Dr. Olivier DEBAUCHE, Senior Researcher at Department of Computer Science, Faculty of Engineering, University of Mons, Belgium; for his unconditional support on the computing and calculation processes of this research.

- Dr. Arnaud J TEMME, Associate Professor at Department of Geography and Geospatial Sciences, Kansas State University, USA; for his guidance and direction on the reasoning process, to tackle the current work, and find out an equilibrium between what is desired to be published and the availability of our data.
- Dr. Omar F. ALTHUWAYNEE, Post-doctoral Fellow at Department of Energy and Mineral Resources Engineering, Sejong University, South Korea; for granting free access to his online course to test our results.

References

- Ait Brahim, L., & Soussey, A. F. (2003). Utilisation de la télédétection pour l'analyse de la fracturation du domaine interne Rifain (Maroc): Relation avec la répartition des sources. *Télédétection*, 1, 33–47.
- Ait Brahim, L., Chotin, P., Hinaj, S., Abdelouafi, A., El Adraoui, A., Nakcha, C., Dhont, D., Charroud, M., Alaoui, F. S., Amrhar, M., & Bouaza, A. (2002). Paleostress evolution in the Moroccan African margin from Triassic to present. *Tectonophysics*, 357(1–4), 187–205.
- Chen, W., Yan, X., Zhao, Z., Hong, H., Bui, D. T., & Pradhan, B. (2019). Spatial prediction of landslide susceptibility using data mining-based kernel logistic regression, naive Bayes and RBF network models for the Long County area (China). *Bulletin of Engineering Geology and the Environment*, 78(1), 247–266.
- Ciampalini, A., Bardi, F., Bianchini, S., Frodella, W., Del Ventisette, C., Moretti, S., & Casagli, N. (2014). Analysis of building deformation in landslide area using multisensor PSInSAR™ technique. *International Journal of Applied Earth Observation and Geoinformation*, 1(33), 166–180.
- Corona, C., Lopez-Saez, J., Favillier, A., Mainieri, R., Eckert, N., Trappmann, D., Stoffel, M., Bourrier, F., & Berger, F. (2017). Modeling rockfall frequency and bounce height from three-dimensional simulation process models and growth disturbances in submontane broadleaved trees. *Geomorphology*, 15(281), 66–77.
- Elmoulat, M., & Ait Brahim, L. (2018). Landslides susceptibility mapping using GIS and weights of evidence model in Tetouan-Ras-Mazari area (Northern Morocco). *Geomatics, Natural Hazards and Risk*, 9(1), 1306–1325.
- Elmoulat, M., & Ait Brahim, L. (2020). Landslides susceptibility assessment using frequency ratio method, remote sensing datasets, and GIS-based techniques. In D. S. Krogh (Ed.), *Landslides: Monitoring, susceptibility and management* (pp. 69–114). Nova Science Publishers, Inc.
- Elmoulat, M., Brahim, L. A., Mastere, M., & Jemmah, A. I. (2015). Mapping of mass movements susceptibility in the Zoumi region using satellite image and GIS technology (Moroccan Rif). *International Journal of Scientific & Engineering Research*, 6(2), 210–217.
- Haut-commissariat au Plan. (2014). *Note sur les premiers résultats du Recensement Général de la Population et de l'Habitat*. <https://www.hcp.ma/>. Accessed 30 Mar 2021.
- Kassab, A. (1976). Agriculture et ressources en eau en Kroumirie. IV Coll. *Géogr. maghrébine, Tunis. Cah du C.E.R.E.S.*, 207–220.
- Kassab, A. (1979). L'homme et le milieu naturel dans les régions de Sejnane et de Tabarca. *Méditerranée*, 3e sér, 35, 39–46.
- Kim, J. C., Lee, S., Jung, H. S., & Lee, S. (2018). Landslide susceptibility mapping using random forest and boosted tree models in Pyeong-Chang, Korea. *Geocarto international*, 33(9), 1000–1015.
- Kirat, M. (1993). *Essai de cartographie géomorphologique et étude des mouvements de terrain dans la vallée de l'Oued El Kbir (Province de Tetouan, Rif occidental: Maroc Septentrional)* [Test of geomorphological mapping and movement study of ground in the valley of the Wadi El Kbir (Province of Western Tetouan)] [dissertation]. Lille: University of Sciences and Technology of Lille I.

- Lee, S. (2019). Current and future status of GIS-based landslide susceptibility mapping: A literature review. *Korean Journal of Remote Sensing*, 1(264), 109–117. <https://doi.org/10.7780/kjrs.2019.35.1.12>
- Mansour, M., & Ait Brahim, L. (2005). Apport de la télédétection Radar et du MNT à l'analyse de la fracturation et la dynamique des versants dans la région de Bab Taza, Rif. *Maroc. Télédétection*, 5, 95–103.
- Marthelot, P. (1957). L'érosion dans la montagne kroumir. *Revue de géographie alpine*, 273–287.
- Marthelot, P. (1959). Note sur un décollement de versant dans la vallée des Atatfa (Kroumirie). *Actes du 84e Congrès national des sociétés savantes, Dijon Section de Géographie*, 61–65.
- Mastere, M., Lanoë, B. V., Brahim, L. A., & El Moulat, M. (2015). A linear indexing approach to mass movements susceptibility mapping-the case of the Chefchaouen province (Morocco). *Revue internationale de géomatique.*, 25(2), 245–265.
- Mate. (2004). *Rapport national de l'Algérie sur la mise en œuvre de la Convention de Lutte Contre la Désertification*. Algérie: Ministère de l'agriculture et du développement rural. www.unccd-prais.com. Accessed 30 Mar 2021.
- Maurer, G. (1976). Les mouvements de masse dans l'évolution des versants des régions telliennes et Rifaines d'Afrique du Nord. Actes du Symposium sur les versants en pays méditerranées 1976. *Provence.C.E.G.R.M, Suppl*, 133–137.
- Maurer, G. (1979). Les milieux naturels et leur aménagement dans les montagnes humides du domaine Rifain et tellien d'Afrique du Nord. *Méditerranée*, 47–56.
- Nemcova, P. (2021). <https://www.quoteswave.com/>. Accessed 29 Mar 2021.
- Nicu, I. C. (2017). Frequency ratio and GIS-based evaluation of landslide susceptibility applied to cultural heritage assessment. *Journal of Cultural Heritage*, 28, 172–176.
- Pateau, M. (2014). De l'aléa au risque naturel: cas de la région Tanger-Tétouan (Rif, Maroc). *Geo-Eco-Trop*, 1, 23–32.
- Shi, J. S., Wu, L. Z., Wu, S. R., Li, B., Wang, T., & Xin, P. (2016). Analysis of the causes of large-scale loess landslides in Baoji. *China. Geomorphology.*, 264, 109–117.
- Zhou, S., Chen, G., Fang, L., & Nie, Y. (2016). GIS-based integration of subjective and objective weighting methods for regional landslides susceptibility mapping. *Sustainability*, 8(4), 334.